JOURNAL OF MATERIALS SCIENCE 26 (1991) 4818–4822

Reduction reaction of lanthanum-added cerium dioxide with carbon monoxide

M. OZAWA, M. KIMURA, A. ISOGAI
Toyota Central Research and Development Laboratories, Inc., Nagakute, Aichi 480-11, Japan

The reaction of lanthanum-added cerium dioxide with carbon monoxide was examined by using a CO pulse reaction method and high-temperature X-ray diffraction (XRD). The lanthanum addition enhanced the activity of cerium dioxide for oxidizing carbon monoxide under moderately reducing conditions. Isothermal XRD observation at 500 and 700 °C indicated that the reduction reaction of CeO_2 and La-added CeO_2 with CO progressed in CO–N_2 flowing gas. The kinetics of the reaction $CeO_2 + \frac{x}{2}CO \rightarrow Ce^{4+}_{1-x}Ce^{3+}_{x}O_{2-\frac{x}{2}} + \frac{x}{2}CO_2 + \frac{x}{2}V_O$ was analysed by Jander's model: $[1 - (1 - x)^{1/3}]^2 = kt$.

1. Introduction

Cerium dioxide (CeO_2) is one of the non-stoichiometric oxides [1], and has been often used as a promoter in an automotive exhaust catalyst for purifying carbon monoxide (CO), nitrogen oxides (NO_x) and hydrocarbon (HC) [2–8]. The automotive catalyst system has been operated under the conditions of a certain range of air/fuel ratio (A/F), which is controlled by an oxygen sensor device, so that it has the highest purifying activities. The role of cerium dioxide is called an oxygen storage effect [2–6], which can suppress the fluctuation of A/F in exhaust gas from automotive engines. Cerium dioxide can provide oxygen for oxidizing CO and HC under rich A/F conditions, and remove it from the exhaust gas phase for reducing NO_x under lean A/F conditions. Ce^{4+} in the CeO_2 lattice easily changes to Ce^{3+}, i.e. CeO_2 is reduced to $CeO_{2-x}(Ce^{4+}_{1-x}Ce^{3+}_{x}O_{2-(x/2)})$ with a reducing gas such as CO, because of the low redox potential.

In previous work on an automotive catalyst [9, 10], we have reported that the addition of lanthanum in an automotive catalyst containing cerium improved the initial three-way (CO, NO_x, HC) activities and the durability of the catalyst. It has been suggested that La improves the thermal stability of the alumina support and enhances the oxygen storage activity in cerium dioxide. In this study the reduction reaction of La-added CeO_2 with carbon monoxide was investigated by using a CO pulse reaction method and high-temperature X-ray diffraction, and is discussed with reference to the kinetics and non-stoichiometry.

2. Experimental procedure

2.1. Samples

The starting cerium dioxide powder was prepared by pyrolysis of cerium nitrate at 600 °C for 3 h. La addition to CeO_2 was done by the impregnation technique using aqueous lanthanum nitrate. The samples were dried at 110 °C for 8 h and heated in air at 600 °C for 3 h. Powders of CeO_2 and La-added CeO_2 were further heated in air at 800 °C for 15 h and used for X-ray diffraction study. The surface area was 15 $m^2 g^{-1}$ for CeO_2, 25 $m^2 g^{-1}$ for $(CeO_2)_{0.9}$-$(LaO_{1.5})_{0.1}$ and 30 $m^2 g^{-1}$ for $(CeO_2)_{0.8}(LaO_{1.5})_{0.2}$. CeO_2 powder with a surface area of 50 $m^2 g^{-1}$ was also prepared by heating at 700 °C for 5 h.

2.2. CO pulse reaction experiments

Pulse reaction experiments were carried out using the pulse reaction apparatus attached to a mass filter detector. The amount of samples used was 0.5 g and purified helium was used as a carrier gas. The samples were pre-heated in oxygen up to 800 °C at 10 K min^{-1}, held at 800 °C for 30 min and cooled down to room temperature. The gas was then changed to helium and the samples held for 30 min. The pulse injection of carbon monoxide was done with a pulse interval of 3 min and an amount of 8 μmol, under conditions of heating the sample at 8 K min^{-1} up to 600 °C and then holding it at 600 °C for 25 min. CO_2 was detected with a mass filter and the CO pulse was monitored with a gas chromatograph detector.

2.3. High-temperature X-ray diffraction (HT-XRD) experiments

X-ray diffraction data were recorded by a powder X-ray diffractometer (Rigaku, RU-200B) with a monochromator, CoK_α X-ray source of 40 kV and 180 mA, and high-temperature measurement cell. Powder samples were arranged on a plate with a heater. The programme of heating and gas introduction was as follows:

1. A sample is heated up to 500 or 700 °C at the heating rate of 8 K min^{-1} in flowing 4% O_2–N_2.

0022–2461/91 $03.00 + .12

2. It is held at 500 or 700 °C and then the gas is changed to N_2 to purge O_2 for 30 min, and 8% CO–N_2 is introduced in the cell.

3. It is cooled down to room temperature in 8% CO–N_2.

The amount of flowing gas was 200 ml min^{-1} and the soaking time was about 150 min. The variation of diffraction angle in the (3 1 1) diffraction line of the fluorite structure was measured with a scanning rate of $2\theta = 2° \, min^{-1}$ during high-temperature experiments. The temperature was monitored by a Pt–Rh thermocouple inserted in the sample on a plate. Phase analysis of the powders was also done by the same apparatus.

3. Results and discussion

Powder X-ray diffraction of the samples detected the cubic fluorite structure with a lattice constant of 0.5411 nm for CeO_2, 0.5420 nm for $(CeO_2)_{0.9}(LaO_{1.5})_{0.1}$ and 0.5422 nm for $(CeO_2)_{0.8}(LaO_{1.5})_{0.2}$, increasing with larger La content. However, the amount of variation in lattice constant with La addition was smaller than that reported in the literature [11, 12]. This indicates the formation of surface-modified CeO_2 with La instead of complete solid solution, because of the heat treatment at low temperature.

Fig. 1 shows the CO pulse experiment results for CeO_2 and $(CeO_2)_{0.9}(LaO_{1.5})_{0.1}$, and indicates the relation of CO oxidation conversion to CO_2 at temperatures up to 600 °C and the pulse number at 600 °C. CO oxidation activity appeared above 380 °C for CeO_2 and above 450 °C for $(CeO_2)_{0.9}(LaO_{1.5})_{0.1}$, and increased with elevating temperature. The conversion, normalized by the powder specific surface area for CeO_2, was larger than that for $(CeO_2)_{0.9}(LaO_{1.5})_{0.1}$ below 550 °C, but at 600 °C this was reversed. The isothermal data at 600 °C showed that the conversion decreased with the pulse number, and the amount of the decrease in conversion was larger for CeO_2 than for $(CeO_2)_{0.9}(LaO_{1.5})_{0.1}$. The results indicate that La addition enhances the oxidation activity of CeO_2 after being moderately reduced, whereas it suppresses the activity at low temperature. No activity for CO oxidation was observed for completely reduced CeO_2 powders, heated in H_2 gas at 800 °C for 5 h. This suggests that oxygen for CO oxidation was supplied from the CeO_2 lattice and that La enhanced the supply of lattice oxygen to the surface in CeO_2 under moderately reducing conditions.

Fig. 2 shows the observed isothermal X-ray results indicating the variation in 2θ of the (3 1 1) diffraction line under the conditions of changing N_2 to CO–N_2 at 700 °C for CeO_2 and $(CeO_2)_{0.8}(LaO_{1.5})_{0.2}$. The diffraction lines were shifted to lower angles, i.e. the (3 1 1) plane separation increased with soaking time in CO–N_2. The amount of shift in 2θ with time increased as a larger content of La was added to CeO_2.

Fig. 3 shows the variation of lattice constants for CeO_2 and $(CeO_2)_{0.8}(LaO_{1.5})_{0.2}$, calculated from (3 1 1) diffraction lines under the conditions described earlier, i.e. being heated up to 700 °C in flowing 4% O_2–N_2 and cooled down from 700 °C to room temperature in 8% CO–N_2 after being soaked in 8% CO–N_2 for 150 min. The thermal expansion coefficient was obtained as $1.2 \times 10^{-5} \, deg^{-1}$ for CeO_2 and $(CeO_2)_{0.8}(LaO_{1.5})_{0.2}$ from heating data in 4% O_2–N_2. On being cooled in 8% CO–N_2 the lattice constants were found to show a non-linear change, with breaks at 600 °C for CeO_2 and at 550 °C for $(CeO_2)_{0.8}(LaO_{1.5})_{0.2}$. The cooling data became the same as for heating data below 300 °C. It was observed that the lattice constant of CeO_2 began to decrease when the CO–N_2 gas was replaced by N_2 and it became the same as the value in O_2–N_2. This result is explained by the reoxidation of reduced CeO_2 by oxygen slightly contaminating the N_2 gas used. CO pulse reaction data indicated that CeO_2 and La-added CeO_2 had a reaction activity increasing with elevating temperature above 380 and 450 °C but did not react with CO below 350 and 420 °C, respectively. It is considered that the data for the lattice constant on cooling are influenced by the reaction activity of CeO_2 with CO. If the activity is higher, the oxide is moderately reduced by CO so that its lattice constant is larger. The non-linear variation in the cooling data can be explained by the temperature dependence of the reaction activity of oxygen supplied from the CeO_2 lattice with CO in the gas phase.

The relation of the lattice constant with time as shown in Fig. 3 will make it possible to discuss the

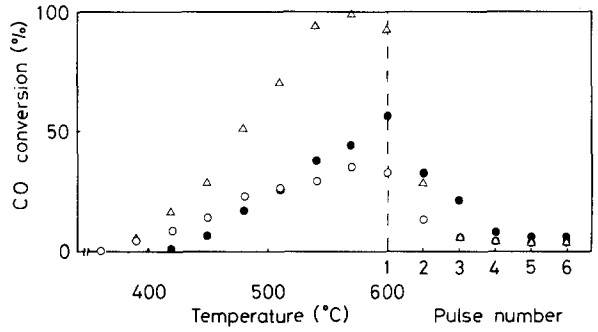

Figure 1 The relation of CO pulse conversion with temperature and pulse number at 600 °C for (Δ) CeO_2 with 50 $m^2 \, g^{-1}$, (○) CeO_2 with 15 $m^2 \, g^{-1}$ and (●) $(CeO_2)_{0.9}(LaO_{1.5})_{0.1}$ with 25 $m^2 \, g^{-1}$.

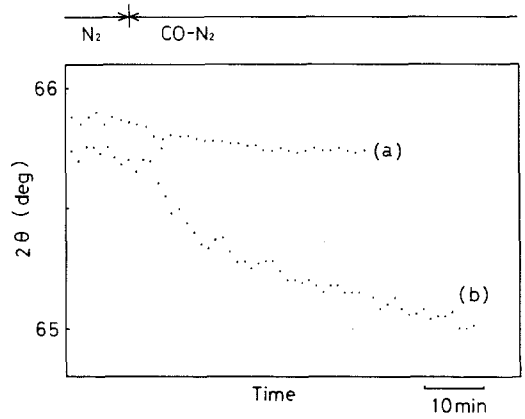

Figure 2 The variation of diffraction angle 2θ in (3 1 1) diffraction lines on changing flowing gas of N_2 to 8% CO–N_2 at 700 °C for (a) CeO_2 and (b) $(CeO_2)_{0.8}(LaO_{1.5})_{0.2}$.

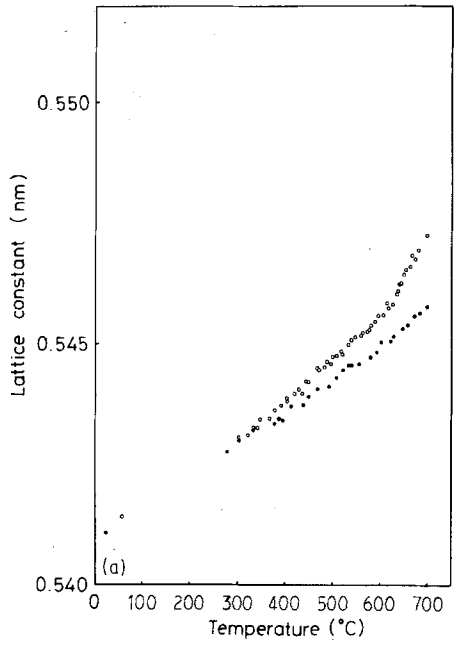

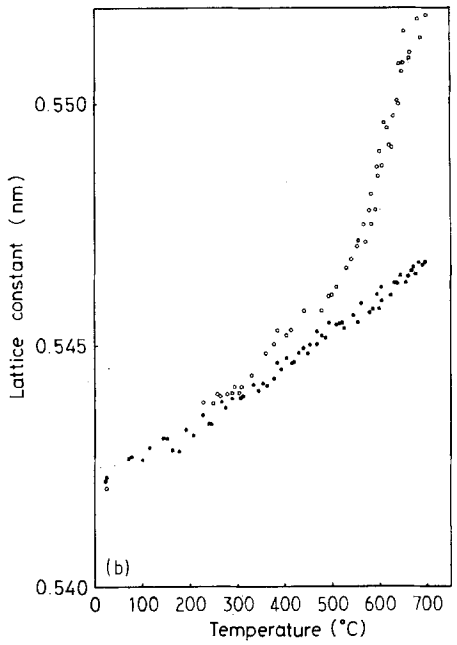

Figure 3 The dependence of lattice constant on temperature for (a) CeO_2 and (b) $(CeO_2)_{0.8}(LaO_{1.5})_{0.2}$: (●) heating in 4% O_2–N_2, (○) cooling in 8% CO–N_2.

reaction kinetics of the reduction of CeO_2 with CO. The CO oxidation activity of CeO_2 is considered to be due to the lattice oxygen O_L which diffuses from the inner part to the surface of a CeO_2 particle. A lattice oxygen atom reacts with a CO molecule adsorbed on the surface from the gas phase, and CO_2 and oxygen vacancy V_O form on the surface. After CO_2 is removed to the gas phase, a newly adsorbed CO molecule on the surface will react with another lattice oxygen supplied from the inner part of CeO_2 again. Here the lattice oxygen diffuses to the surface, whereas the oxygen vacancy does so from the surface into the particle. The total mass transport in the reaction is illustrated in Fig. 4. The reaction is written as

$$CeO_2 + \frac{x}{2}CO \rightarrow Ce^{4+}_{1-x}Ce^{3+}_{x}O_{2-\frac{x}{2}} + \frac{x}{2}CO_2 + \frac{x}{2}V_O \quad (1)$$

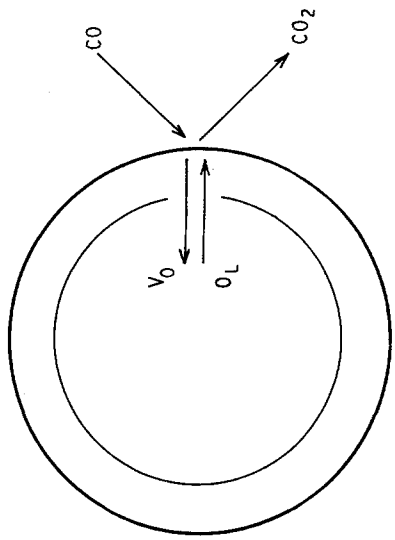

Figure 4 Mass transport model in the reaction of CeO_2 with CO.

For the reaction in this work, Jander's model [13] on solid–gas reaction can be adapted under the following assumptions:

1. A sphere-shaped particle is surrounded by the reaction gas component with a certain concentration.
2. Reaction progresses from the surface to the inner part of a particle with sphere–shell shape.
3. Reaction is controlled by the diffusion process in the solid.
4. The particle size is constant before and after reaction.

In the case of the reduction reaction of CeO_2 with CO, CO will easily react with lattice oxygen and the amount of CO_2 formed in the reaction is equal to that of oxygen vacancy in the CeO_2 lattice, so that the reaction $CO + xO_L \rightarrow xCO_2$ will be able to be replaced by the reaction $CeO_2 \rightarrow CeO_{2-x} + xV_O$. The Jander reaction kinetics is represented as

$$[1 - (1 - x)^{1/3}]^2 = kt \quad (2)$$

Here x is the fraction reacted, k the rate constant and t is time. As represented by Equation 1, the reduction reaction is due to the change of Ce^{4+} to Ce^{3+} in the CeO_2 lattice. When Ce^{4+} changes to Ce^{3+} with reacted fraction x in the lattice, the plane-distance d increases according to

$$d = d_0\left(1 + \frac{x\Delta r}{r}\right) \quad (3)$$

Here d_0 is the plane-distance in CeO_2 before the reaction. Δr is the amount of the increase in the bond length between Ce ion and oxide ion, $r = r_{Ce_4^+} + r_{O_2^-}$; $\Delta r = r_{Ce_3^+} - r_{Ce_4^+}$. $r_{Ce_4^+}$, $r_{Ce_3^+}$ and $r_{O_2^-}$ are ionic radii of the ions Ce^{4+}, Ce^{3+} and O^{2-}, and are 0.102, 0.118 and 0.132 nm, respectively from Goldshumitt [14, 15].

Fig. 5a–c shows the relations of x versus t observed at 700 °C for CeO_2, $(CeO_2)_{0.9}(LaO_{1.5})_{0.1}$ and $(CeO_2)_{0.8}(LaO_{1.5})_{0.2}$ respectively. The solid lines show the results calculated using Equation 1 with the value of $k = 4.1 \times 10^{-8}\,s^{-1}$ for Fig. 5a, $1.9 \times 10^{-7}\,s^{-1}$ for Fig. 5b and $7.1 \times 10^{-7}\,s^{-1}$ for Fig. 5c. The same

TABLE I Kinetic constant, k and k_s (normalized with surface area) for CeO_2 and La-added CeO_2

Compound	700 °C		500 °C	
	k (s^{-1})	k_s ($s^{-1}m^{-2}g$)	k (s^{-1})	k_s ($s^{-1}m^{-2}g$)
CeO_2	4.1×10^{-8}	2.7×10^{-9}	–	–
$(CeO_2)_{0.9}(LaO_{1.5})_{0.1}$	1.9×10^{-7}	7.7×10^{-9}	7.2×10^{-9}	2.9×10^{-10}
$(CeO_2)_{0.8}(LaO_{1.5})_{0.2}$	7.1×10^{-7}	2.4×10^{-8}	2.8×10^{-8}	9.4×10^{-10}

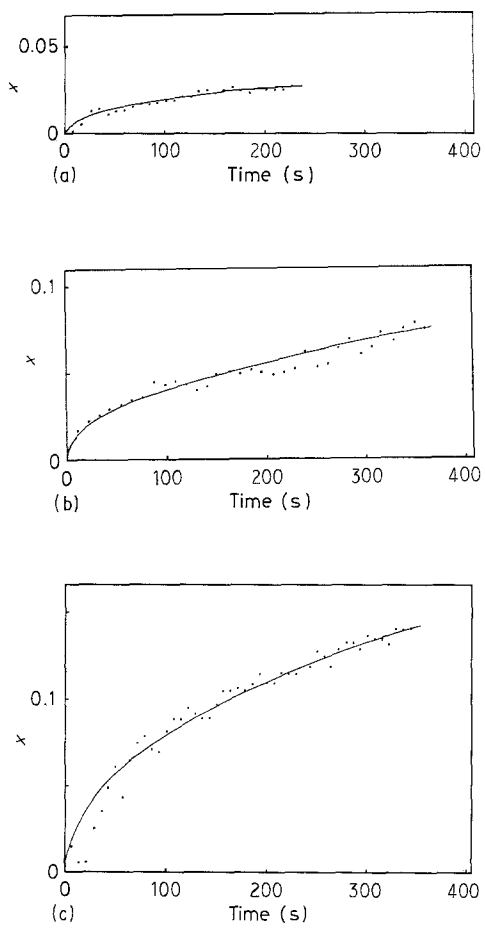

Figure 5 The relation of reacted fraction x versus time t at 700 °C for (a) CeO_2, (b) $(CeO_2)_{0.9}(LaO_{1.5})_{0.1}$ and (c) $(CeO_2)_{0.8}(LaO_{1.5})_{0.2}$. Solid lines are the relation calculated by the kinetics equation: $[1-(1-x)^{1/3}]^2 = kt$. The value of k is $4.1 \times 10^{-8} s^{-1}$ for (a), $1.9 \times 10^{-7} s^{-1}$ for (b) and $7.1 \times 10^{-7} s^{-1}$ for (c).

procedure was used for the 500 °C isothermal data. The data for CeO_2 at 500 °C could not be calculated because of the small amount of variation in the d value. The derived k constants are listed in Table I. They were further normalized by powder surface area using the relation $k = k_s \cdot S$ (k_s = normalized rate constant, S = surface area), and values are also listed in Table I. The reaction activity of CeO_2 was enhanced by La addition ca.3 times for $(CeO_2)_{0.9}(LaO_{1.5})_{0.1}$ and ca. 9 times for $(CeO_2)_{0.8}(LaO_{1.5})_{0.2}$ at 700 °C. The total amount of lattice oxygen diffusing in CeO_2 and reacting with CO is dependent on the concentration of the oxygen vacancy. Since La doping in CeO_2 produces oxygen vacancy in the lattice by forming $Ce_{1-x}La_xO_{2-(x/2)}$, La addition is effective for the promotion of the reaction of CeO_2 with carbon monoxide.

The phenomenon seems to be similar to the oxide ion conduction of fluorite-type oxides including $Ce_{1-x}M_xO_{2-(x/2)}$ and $Zr_{1-x}M_xO_{2-(x/2)}$ (M = rare earths). Both processes are controlled by the diffusion of oxygen vacancy; the ion conduction is activated by an electric field, whereas the reduction reaction of CeO_2 is done by removing oxygen with carbon monoxide on the surface. The conductivity σ at constant dopant concentration depends on the temperature T and is often written as $\sigma = (\sigma_0/T)\exp(-E/RT)$, where E is the activation energy of σ and σ_0/T is a pre-exponential term. If the reaction is due to the diffusion of oxygen vacancy as for ionic conduction, the relation of σ versus E can be replaced by k versus E. The E value derived from the data at 500 and 700 °C in this work was 1.1×10^5 J mol^{-1} for both $(CeO_2)_{0.9}(LaO_{1.5})_{0.1}$ and $(CeO_2)_{0.8}(LaO_{1.5})_{0.2}$. It is a reasonable value as an activation energy of diffusion of oxygen vacancy, considering La segregation on the surface of the samples used and the data on ionic conduction in earlier references: E = 87–91 kJ mol^{-1} (0.90–0.94 eV) at $x = 0.3$ for $(CeO_2)_{1-x}(LaO_{1.5})_x$ [16–18], 70 kJ mol^{-1} (0.73 eV) at $x = 0.2$ and 128 kJ mol^{-1} (1.33 eV) at $x = 0.4$ for $(CeO_2)_{1-x}(GdO_{1.5})_x$ [19]. The results suggest that La addition to CeO_2 promotes the diffusion of oxygen vacancy and surface reaction with CO in CeO_2 under moderately reducing condition. It is expected that La-added CeO_2 is more effective than CeO_2 for suppressing the A/F fluctuation in an automotive catalyst.

4. Conclusion

CO pulse and HT-XRD data indicated that lanthanum addition enhanced the CO oxidation activity of cerium dioxide under moderately reducing condition. The reaction kinetics of reduction of CeO_2 and La-added CeO_2 was discussed with isothermal HT-XRD data at 500 and 700 °C. The results were explained by Jander's kinetics:

$$[1-(1-x)^{1/3}]^2 = kt.$$

Acknowledgement

The authors would like to thank Mr H. Shinjouh for operation of the CO pulse apparatus.

References

1. D. J. M. BEVEN and J. KORDIS, *J. Inorg. Nucl. Chem.* **26** (1964) 1509.

2. H. S. GANDHI, A. G. PIKEN, M. SHELEF and R. G. DOLOSH, SAE paper No. 760201 (Society of Automotive Engineers, Warrendale, Pennsylvania, 1976).
3. Y. F. YU-YAO and J. T. KUMMER, *J. Catal.* **106** (1987) 307.
4. H. C. YAO and Y. F. YU-YAO, *ibid.* **86** (1984) 254.
5. E. C. SU, C. N. MONTREUIL and W. G. ROTHSCHILD, *Appl. Catal.* **17** (1985) 75.
6. R. K. HERZ and J. A. SELL, *J. Catal.* **94** (1985) 166.
7. J. C. SCHLATTER and P. J. MITCHELL, *Ind. Eng. Chem. Res. Dev.* **19** (1980) 288.
8. G. KIM, *ibid.* **21** (1982) 267.
9. N. MIYOSHI, S. MATSUMOTO, M. OZAWA and M. KIMURA, SAE paper No. 891970 (Society of Automotive Engineers, Dearborn, Michigan, 1989).
10. S. MATSUMOTO, N. MIYOSHI, T. KANAZAWA, M. KIMURA and M. OZAWA, "Catalytic Science and Technology Vol. 1, edited by S. Yoshida, N. Tabezawa and T. Ono (Kodansha, Tokyo, VCH; New York, 1991) p. 335.
11. E. ZINTL and U. CROATTO, *Z. anorg. allgem. Chem.* **242** (1939) 79.
12. T. TAKAHASHI and H. IWAHARA, *Denki Kagaku* **34** (1966) 906.
13. W. JANDER, *Z. anorg. allgem. Chem.* **163** (1927) 1.
14. V. M. GOLDSCHMIDT, "Geochemische Verteilungsgesetze der Elemente", (Skrifter Nerske Videnskarp-Akad., Oslo, 1926).
15 L. PAULING, "The nature of the chemical bond" (Cornell University, Cornell, 1960).
16. T. KUDO and H. OBAYASHI, *J. Electrochem. Soc.* **122** (1975) 142.
17. R. T. DIRSTINE, R. N. BLUMENTHAL and T. F. KEUCH, *ibid.* **126** (1979) 264.
18. W. E. ARMSTRONG and D. L. TOLLIVER, *ibid.* **121** (1974) 307.
19. T. KUDO and H. OBAYASHI, *ibid.* **123** (1976) 415.

Received 23 April 1990
and accepted 15 January 1991